Supplemental Information

Materials and Methods

Animals

ENT1$^{-/-}$ mice were generated as described (1). We used F2 generation hybrid mice with a C57BL/6J × 129X1/SvJ genetic background to minimize the risk of false positives or negatives in behavioral phenotypes that could be influenced by a single genetic background (2). CRE-LacZ mice were generated by Dr. Jerry Yin (University of Wisconsin) and provided by Dr. Eric Nestler (Mount Sinai School of Medicine) (3). We crossed CRE-lacZ mice in a C57BL/6J background with ENT1$^{-/-}$ mice in a C57BL/6J background, then crossed the CRE-lacZ/ENT1$^{+/-}$ with ENT1$^{+/-}$ mice in a 129X1/SvJ background to generate CRE-lacZ/ENT1$^{+/+}$ or CRE-lacZ/ENT1$^{-/-}$ mice. We used 8-16 week old male littermates for experiments. Mice were housed in standard Plexiglas cages with food and water *ad libitum*. The colony room was maintained on a 12 h light/12 h dark cycle with lights on at 6:00 a.m. Animal care and handling procedures were approved by the Mayo Clinic Institutional Animal Care and Use Committees in accordance with NIH guidelines.

Measurement of Extracellular Adenosine or Glutamate Levels Using Microdialysis

Adenosine and Glutamate Microdialysis: To analyze possible changes in extracellular adenosine or glutamate owing to the deletion of ENT1, we employed a microdialysis and LC/MS/MS method. Animals were anesthetized with ketamine/xylazine (100 and 15 mg/kg, *i.p.*; Sigma, St. Louis, MO) and placed in a digital stereotaxic alignment system (Model 1900, David Kopf Instruments, Tujunga, CA). After the skull was exposed, the mouse was positioned with

the bregma at the focal point, and the skull was leveled using a dual-tilt measurement tool. 0.5 mm diameter holes were drilled for placement of the guide cannula. A guide cannula for microdialysis was implanted into the nucleus accumbens (AP: 1.3 mm; ML: 0.5 mm; DV: -3.5 mm; Figure S1A in Supplement 1 for the location of microdialysis probes) as described (4). Mice were given 7 d for recovery. A 1.0 mm microdialysis membrane (MW cut off: 50,000 Da, Eicom, Kyoto, Japan) was inserted and secured to the guide cannula and standard solutions in Ringer's solution (145 mM NaCl, 2.7 mM KCl, 1.2 mM $CaCl_2$, 1.0 mM $MgCl_2$, pH 7.4) was circulated in the microprobe. After a 2-3 h stabilization period, 20 min fractions were collected for 100 min at a 1.0 μl/min flow rate. The location of the microdialysis probe was confirmed using hematoxylin and eosin (H&E) staining (Figure S1A). The dialysate was desalted and concentrated using Oasis HLB sample cartridges (1 cc, Waters Corp., Milford, MA) up to 20 μl. The dialysates were quantified using UPLC (Waters Corp.) coupled with a TSQ Quantum Ultima MS triple quadrupole mass spectrometer (Thermo Fisher Scientific, Waltham, MA). Separation was performed with Atlantis dC18 NanoEase Columns (3 μm, 300 μm x 100 mm) with a 5 μl/min flow rate. For the screening of adenosine, multiple reactions monitoring (MRM) was programmed to detect 136 (m/z) unique fragments from the adenosine parent ion (M.W. 268) under 20 eV collision energy. Also, both the 84 (m/z) fragment and the 130 (m/z) fragment (fragmented by 18 eV and 10 eV, respectively) were measured to analyze the glutamate level from the glutamate parent ion (M.W. 147). The dialysate concentration was determined using calibration curves at a range of 0.1 - 100 ng/μl (ppm). Standard calibration and quantification was performed using the Quan browser package in XCalibur 2.0.7 (Thermo Fisher Scientific Inc.).

No-Net Flux Microdialysis: To confirm the extracellular glutamate concentration in the NAc, we employed a no-net flux microdialysis experiment that allowed glutamate to spontaneously diffuse through a microprobe membrane by its concentration gradient (5). A guide cannula was implanted into the nucleus accumbens (AP: 1.3 mm; ML: 0.5 mm; DV: -3.5 mm Figure S1A in Supplement 1 for the location of microdialysis probes) as described (4). Mice were given 7 d for recovery. A 1.0 mm microdialysis membrane (MW cut off: 50,000 Da, Eicom) was inserted and secured to the guide cannula. For the no-net flux experiment, 0, 0.5, 1.0, and 5.0 μM glutamate standard solutions in Ringer's solution (145 mM NaCl, 2.7 mM KCl, 1.2 mM $CaCl_2$, 1.0 mM $MgCl_2$, pH 7.4) were circulated in the microprobe and equilibrated with extracellular glutamate. After a 2-3 h stabilization period, two 20 min fractions per each standard glutamate solution were collected at a 0.6 μl/min flow rate to calculate the *p*-value of each steady-state condition. Glutamate concentrations were quantified using HPLC-ECD (HTEC-500, Eicom) coupled with an autosampler (719D, Alcott, Hamilton Square, NJ). HPLC separation was done using a separation column (GU-GEL, 4.6 × 150 mm, Eicom) and Enzyme column (E-ENZYMPAK, 3 × 4 mm, Eicom), with detection by a platinum electrode detector set at +450 mV (against an Ag/AgCl reference) (WE-PT, Eicom). The mobile phase consisted of 60 mM NH_4Cl-HH_4OH, 250 mg hexadecyltrimethyl ammonium bromide, and EDTA-2Na (0.1 mg/L). Separation was performed at a column temperature of 33ºC with a mobile phase flow rate of 0.4 ml/min. Data were collected through an EPC-500 processor (Eicom), and peak areas were calculated using the PowerChrom software (Eicom). After the microdialysis experiment, we confirmed the location of microdialysis probes histologically.

NAc Protein Profile Using Proteomics

To examine accumbal protein expression changes between ENT1$^{+/+}$ and ENT1$^{-/-}$ mice, we employed an iTRAQ labeling method. Mice were anesthetized with carbon dioxide and rapidly decapitated. NAc tissues were isolated under a surgical microscope. We pooled the same amount of NAc proteins from 5 mice per genotype (10 mice/iTRAQ experiment). We performed three independent iTRAQ experiments with different sets of mice (10 mice/experiment x 3 times) and duplicated each sample for LC/MS/MS analysis. The tissue was homogenized in 50 mM Tris buffer (pH 7.4), 2 mM EDTA, 5 mM EGTA, protease inhibitor, phosphatase inhibitor, and 0.1% SDS. Then, homogenates were centrifuged at 10,000 g for 3 min and the supernatants were collected. To examine endogenous peptides, the tissue was sonicated 3 times at 5W for 5 s in 450 μl of distilled water using Sonic dismembrator model 100 (Fisher Scientific, Pittsburgh, PA) as described (6). Brain extracts were then heated at 70°C for 20 min, cooled on ice, and denatured in 5 mM HCl at room temperature for 10 min. Supernatants were collected after centrifugation at 14,000 g for 2 min. For iTRAQ (Applied Biosystems, Foster City, CA) labeling, the trypsin-digested peptides or endogenous peptides were purified and desalted using an Oasis HLB extraction kit (Waters Corp.) and evaporated in a SpeedVac^{TM} (Eppendorf, Hamburg, Germany). The concentrated peptides were reconstituted in iTRAQ reagents for 2-plex reactions (114 = ENT1$^{+/+}$ mice; 116 = ENT1$^{-/-}$ mice). The iTRAQ-reacted peptides were combined into one tube, further desalted and resolved with a 0.1% formic acid solution. The peptides were loaded into a reverse-phase capillary column (Magic C18, 75 mm x 8 cm; 200 Å) using automated nanoLC system (Eksigent NanoLC system, Dublin, CA). The gradient elution of nanoLC was performed from 5% acetonitrile to 40% acetonitrile in 0.1% formic acid for 2 h. The tandem mass spectrometry (MS/MS) experiment was performed using a LTQ Orbitrap mass

spectrometer (Thermo Fisher Scientific) through FT full scan from 375-1600 m/z with a resolution of 60,000 (at 400 m/z), and then through linear ion trap MS/MS scanning for the top five ions. To enhance iTRAQ acquisition by LTQ Orbitrap, pulsed Q dissociation mode was employed with the following settings; 30 normalized collision energy, 0.55 activation Q, and 0.35 msec activation time (7).

Proteomics and iTRAQ Data Analysis

The MS/MS spectra were compared to a mouse database (Swissprot) using Mascot2.1. (Matrix Science, London, UK) and the iTRAQ modification of lysine residues was set as a fixed modification. The Orbitrap MS data with 5 ppm mass tolerance allowed for intact peptide masses and 0.8 Da was approved for PQD (pulsed Q collision induced dissociation) MS/MS fragmented ions to be detected in the linear ion trap. Through duplicative analysis, 533 proteins were identified, which had at least 3 unique peptides with a CI (confidence interval) > 95% using the Mascot search algorithm (Figure S2A). The iTRAQ reporter ion was quantified using ProteinPilot software^{TM} (Applied Biosystems) and the iTRAQ reaction bias was verified. To validate the experimental variation of each iTRAQ reaction, we spiked 20 pmol of an internal standard peptide (Glu1-Fibrinopeptide B; 1570Da, Sigma). Only iTRAQ labeled samples showing less than 15% bias between 114- and 116-labeled internal standard were selected for iTRAQ quantification (8). In addition, variation in the input protein amount was normalized by a ratio of reporter ions to housekeeping genes, beta-tubulin or GAPDH. After normalization, 27 signaling protein expressions were quantified and analyzed by two-tailed *t*-test. To verify the biological variation of proteins, we also examined accumbal peptide levels (peptidomics) using an iTRAQ method, since many proteomes are processed into peptides. We validated the

processed peptide results with the NAc protein expression results and found overall consistency including those of neurogranin (Figure S2B).

Protein Phosphatase Activity Assay

Cytoplasmic protein (2 μg) from the NAc was used for phosphatase assay (Enzo Life Sciences Inc., Plymouth Meeting, PA). The released phosphates by cellular phosphatase activation were reacted with BIOMOL GREEN™ reagent (Enzo Life Sciences Inc.) and the signal was detected in OD 620 nm using a microplate reader (Thermo Fisher Scientific Inc.). We calculated phosphatase PP1/PP2A activity by subtracting PP2B activity (10 mM EGTA, which is a Ca^{2+} chelator, PP2B inhibitor) from the total phosphatase activity. Similarly, we calculated phosphatase PP2B activity by subtracting PP1/PP2A activity (2.5 mM okadaic acid, which is a PP1/PP2A specific inhibitor) from the total phosphatase activity.

Western Blot Analysis

Mice were anesthetized with carbon dioxide and rapidly decapitated. Brains were quickly removed and dissected to isolate the NAc. Briefly, tissues were homogenized in a solution containing 50 mM Tris buffer (pH 7.4), 2 mM EDTA, 5 mM EGTA, 0.1% SDS, protease inhibitor cocktail (Roche, Indianapolis, IN), and phosphatase inhibitor cocktail type I and II (Sigma). Homogenates were centrifuged at 500 g at 4ºC for 15 min and supernatants were collected. Proteins were analyzed using Bradford protein assay (BioRad, Hercules, CA). Proteins were separated by 4-12% NuPAGE™ Bis Tris gels at 130 V for 2 h, transferred onto PVDF membranes at 30 V for 1 h (Invitrogen, Carlsbad, CA), and incubated with antibodies against NR1 (1:300, AB9864, Millipore, Billerica, MA), phospho-NR1 Ser-890 (1:1000, #3381,

Cell Signaling, Danvers, MA), phospho-NR1 Ser-897 (1:300, #06-641, Millipore), NR2A (1:300, #07-632, Millipore), phospho-NR2A Ser-1232 (1:300, #2056, Tocris, Ellisville, MO), NR2B (1:500, sc-1469, Santa Cruz, Santa Cruz, CA), phospho-NR2B Ser-1303 (1:300, #07-398, Millipore), GluR1 (1:500, #07-660, Millipore), phospho-GluR1 Ser-831 (1:500, #05-823, Millipore), phospho-GluR1 Ser-845 (1:500, AB5849, Millipore), EAAT1 (1:300, sc-7758, Santa Cruz), EAAT2 (1:500, sc-7760, Santa Cruz), CaM (1:1000, #05-173, Millipore), Ng (1:1000, #07-425, Millipore), pNg Ser-36 (1:1000, #07-430, Millipore), PKCγ (1:2000, ab71558, Abcam, Cambridge, MA), phospho-PKCγ Thr-514 (1:1000, #9379, Cell Signaling), CaMKII-pan (1:1000, #3362, Cell Signaling), phospho-CaMKII Thr-286 (1:1000, #3361, Cell Signaling), CREB (1:1000, #9197, Cell Signaling), phospho-CREB Ser-133 (1:1000, #9198S, Cell Signaling), and GAPDH (1:1000, MAB374, Millipore). Blots were developed using chemiluminescent detection reagents (Pierce, Rockford, IL). Chemiluminescent bands were detected on a Kodak Image Station 4000R scanner (New Haven, CT) and quantified using NIH Image J software. Protein levels were normalized by GAPDH and quantified compared to the control group.

X-gal Staining

Using CRE-lacZ/ENT1$^{+/+}$ or CRE-lacZ/ENT1$^{-/-}$ mice, we examined *in vivo* CREB activity. Mice brains were rapidly dissected and incubated in a cold fixative solution (2% paraformaldehyde and 0.2% glutaraldehyde in PBS) and fixed overnight at 4°C. Fixed brain samples were rinsed with PBS and frozen rapidly in mounting medium. Forty μm coronal sections were cut using Leica CM1850 Cryostat (Leica Microsystems, Wetzlar, Germany) and washed for 5 min three times with PBS and incubated overnight at 37°C in a dark tray in the

reaction solution (1 mg/ml X-gal, 5 mM potassium ferricyanide, 5 mM potassium ferrocyanide and 2 mM $MgCl_2$ in PBS). Sections were washed the following day and mounted on Fisherbrand Superfrost Plus microscope slides. Slides were dehydrated, cleared and coverslipped with VectaMount permanent mounting medium. X-gal positive cells were counted in the regions of interest (0.15 mm^2) using a Leica DM4000B microscope.

Microinjection of ENT1 and PKC Inhibitors

Guide cannulae were bilaterally implanted into the NAc (AP: 1.3 mm; ML: ± 1.5 mm; DV: -3.5 mm; Figure S1B in Supplement 1 for the location of microinjection cannula). Mice were given 7 d for recovery. We microinjected into the NAc using microinjection needles (CXMI, Eicom), either 1, 10, 20 μM PKC inhibitor peptide 19-31 (IC_{50} = 100 nM, dissolved in saline; Calbiochem, San Diego, CA) (9), or 50 μM NBTI (dissolved in saline containing 2% dimethyl sulphoxide (DMSO); Sigma), a dose that is known to effectively inhibit ENT1 function in the brain when microinjected as described (10). Because CREB activity is altered 2-3 h after an ethanol injection in the NAc of CRE-lacZ mice (Figure S6 in Supplement 1) which is consistent with CREB-mediated gene expression profile from a recent microarray experiment (11), we examined CREB activity 2 h after an NBTI microinjection. To examine ethanol drinking behaviors, a two-bottle choice drinking experiment was performed as previously described (1, 12). During the experiment, mice were given one week to acclimate to individual housing conditions and handling. Mice were then given 24 h access to two bottles, one containing plain tap water and the other containing an ethanol solution. The concentration of ethanol was raised every 4 d, increasing from 3 to 6 to 10 % (v/v) ethanol in tap water. The positions of the bottles were changed every 2 d to control position preference. Throughout the experiments, fluid intake

and body weight were measured every 2 d using an analytical balance (Denver Instrument, Arvada, CO) with a precision of 0.01 g. Ethanol consumption was expressed as grams of ethanol consumed per kilogram of body weight per day for each mouse. To examine the effect of PKC inhibition on ethanol consumption or preference, a PKC inhibitor was infused using an infusion pump (Harvard Apparatus, Holliston, MA) at a 1 μl/min flow rate in a volume of 1 μl per day. Saline control and PKC inhibitor (1.0 μM, 10 μM and 20 μM) were bilaterally injected for 4 d during the 10% ethanol drinking session. Specifically, to examine the effect of PKC inhibitor on ethanol consumption, fluid intake and body weight were measured every 2 d and the positions of the bottles were changed every 2 d to control position preference. Ethanol consumption was calculated by dividing average ethanol consumption (standardized for evaporation) during each ethanol concentration and saline- or PKC inhibitor-injection periods by the body weight. Ethanol preference ratios were calculated at each ethanol concentration and treatment by dividing the total ethanol solution consumption at each ethanol concentration or treatment (standardized for evaporation) by the total fluid (ethanol plus water) consumption.

Effect of CGP37849 on Signaling Molecules in the NAc and Ethanol Drinking

To examine the effect of CGP37849 (NMDAR-specific antagonist, Tocris) on molecular signaling in the NAc, we used 10 mg/kg of CGP37849 (*i.p.*) based on previous pharmacological and behavioral studies (13, 14). All experiments were performed 2 h following drug administration since we found that CREB activity was reduced in the NAc 2-3 h after ethanol treatment (Figure S6 in Supplement 1) as described above. Furthermore, our previous study (13) has demonstrated that 1-2 h following CGP37849 treatment (10 mg/kg, *i.p.*) was sufficient time to effectively block NMDAR function in mice, which is consistent with another study (15). To

determine the effect of CGP37849 on ethanol drinking, we measured alcohol self-administration using a two-bottle choice experiment as described above. To examine the effect of CGP37849 (NMDAR-specific antagonist, Tocris) on ethanol drinking, a new group of mice was given saline, 1.0, 5.0 and 10 mg/kg CGP37849 (*i.p.*) for 4 d following the 10% ethanol period in a two-bottle drinking experiment.

Statistical Analysis

Data are presented as mean ± SEM (standard error of the mean). Statistical analyses were performed using unpaired two-tailed *t*-test (Prism v 4, GraphPad Software, La Jolla, CA), one-way, or two-way repeated measures ANOVA (SigmaStat v 3.1, Systat Software, Point Richimond, CA). Results were considered significantly different when $p < 0.05$.

Table S1. Protein levels in signaling transduction of the NAc detected by iTRAQ.

Protein ID	Protein	Fold*	S.E.	*p* value**
Q8BH59	*Aralar1*	1.22	0.23	0.346
Q06138	*Cab39*	1.20	0.25	0.475
P11798	*Camk2a*	0.99	0.11	0.671
P28652	*Camk2b*	0.90	0.08	0.420
Q3UHL1	*Camkv*	0.83	0.14	0.172
Q02399	*CDK5*	0.83	0.10	0.335
P56564	*Eaat1*	1.07	0.21	0.877
P15105	*Glns*	0.85	0.13	0.186
P84075	*Hpca*	1.11	0.55	0.792
P63085	*Mapk1*	0.97	0.06	0.501
P31938	*Map2k1*	0.98	0.09	0.667
P47809	*Map2k4*	1.01	0.18	0.890
Q61644	*Pacsin1*	1.44	0.37	0.145
Q61036	*Pak3*	2.14	1.14	0.088
Q61481	*Pde1a*	0.80	0.24	0.210
P62137	*Ppp1ca*	1.00	0.14	0.763
Q60829	*Ppp1r1b*	1.08	0.07	0.843
P63330	*Ppp2ca*	0.73	0.09	0.162
Q76MZ3	*Ppp2r1a*	0.89	0.09	0.225
P58389	*Ppp2r4*	0.76	0.10	0.132
P63328	*Ppp3ca*	0.92	0.08	0.299
P31324	*Prkar2b*	1.15	0.15	0.490
P16858	*Gapdh*	1.04	0.07	0.626
Q7TMM9	*Tubb2a*	0.97	0.05	0.838

*Fold represents expression in ENT1$^{-/-}$ mice compared to ENT1$^{+/+}$ mice.
**By unpaired two-tailed *t*-test.

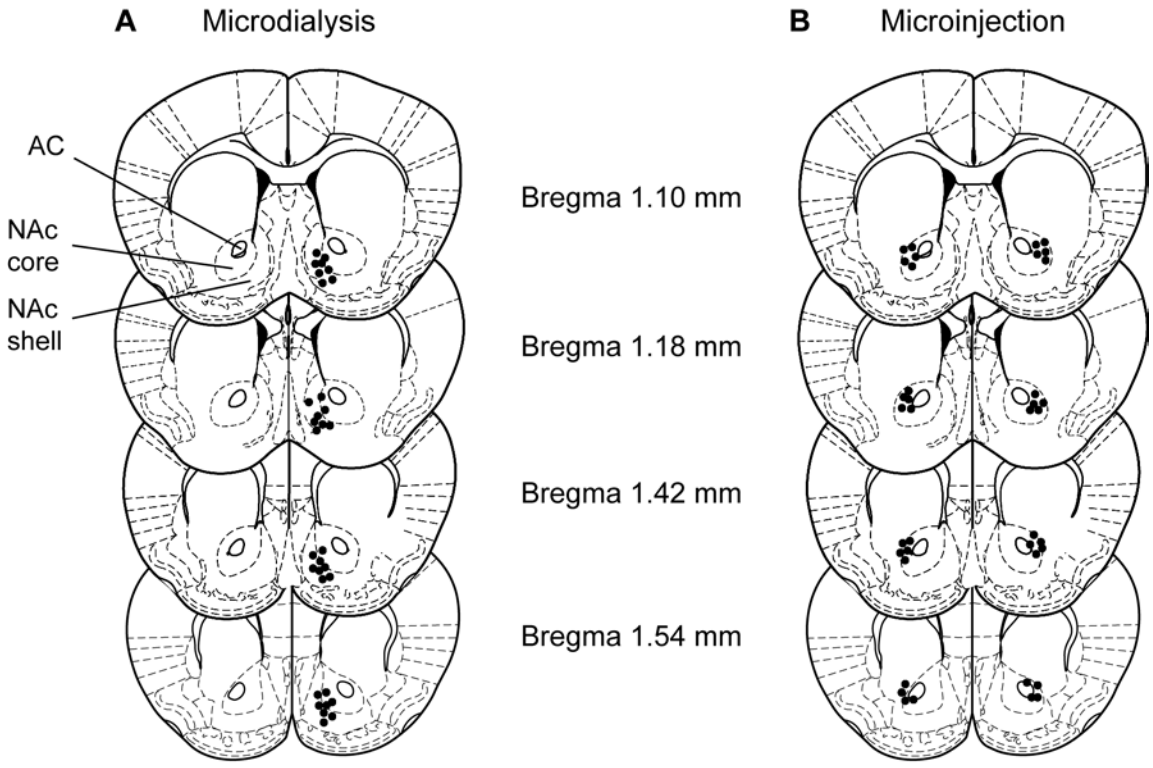

Figure S1. Microdialysis probe and microinjection cannula placements were plotted within the dorsal-medial part of the nucleus accumbens (NAc) including parts of both core and shell regions. **(A)** For microdialysis, AP coordinates were between +1.1 to +1.5 and ML coordinates were between +0.3 to +0.7 from bregma. **(B)** For microinjection, AP coordinates were between +1.1 to +1.5 and ML coordinates were between +1.3 to +1.5 from bregma. Schematic anatomic representation adapted from Paxinos and Franklin's stereotaxic atlas (16) published in *The Mouse Brain in Stereotaxic Coordinates, 3rd edition*, Copyright Elsevier (2008), and reprinted with permission. AC, anterior commissure. All animals with a misplacement of the needle tract or bleeding were excluded from the study.

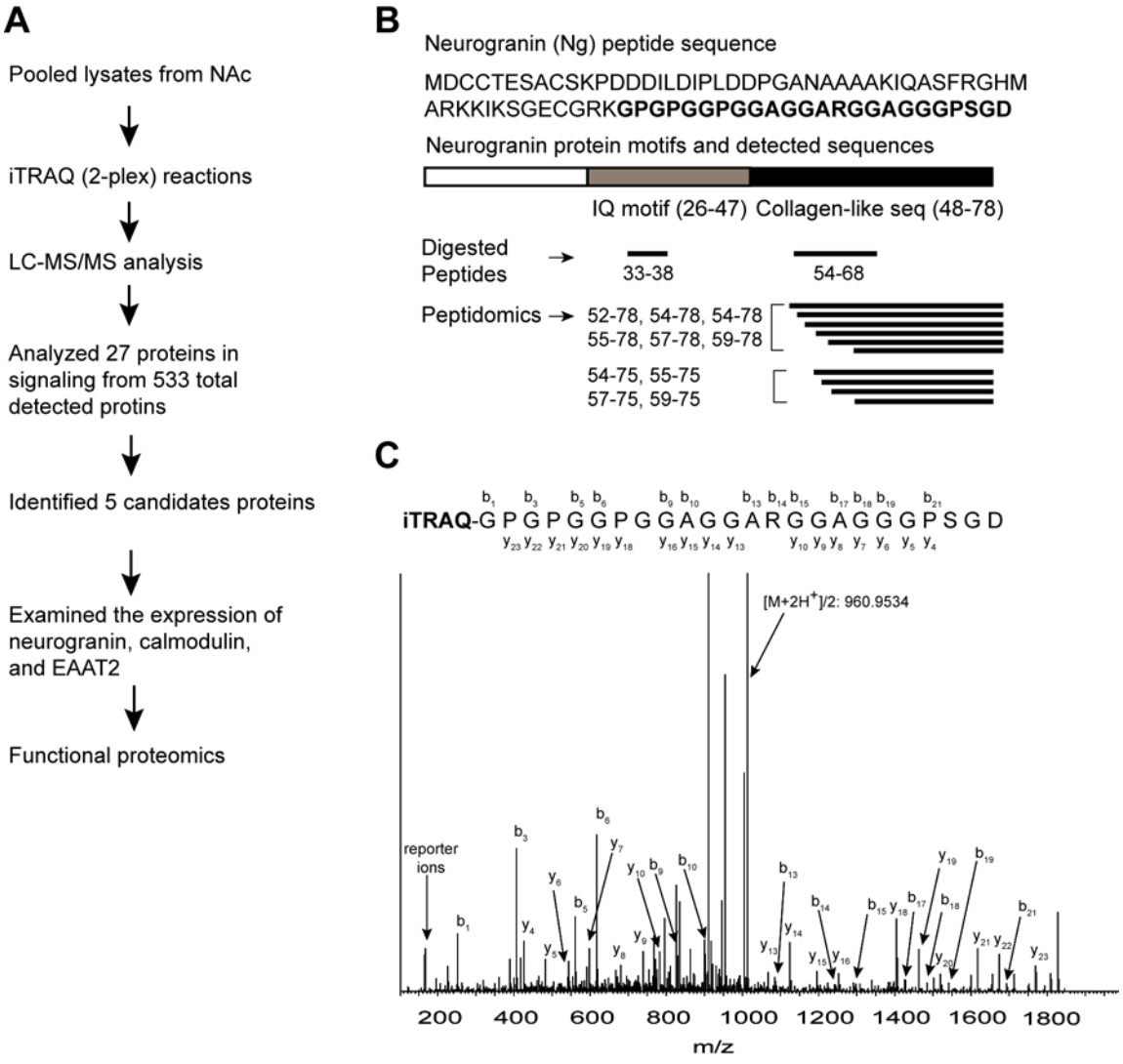

Figure S2. (A) Schematic proteomic analysis procedure of nucleus accumbens (NAc) tissue samples in ENT1$^{-/-}$ mice and ENT1$^{+/+}$ mice. **(B)** The identified peptide sequence of the neurogranin (Ng) and the detected peptides by iTRAQ (bold). Two peptides were detected by trypsin digestion and 10 peptides were detected by peptidomics shown as bold bars. **(C)** Representative MS/MS spectrum of iTRAQ-labeled neurogranin peptide.

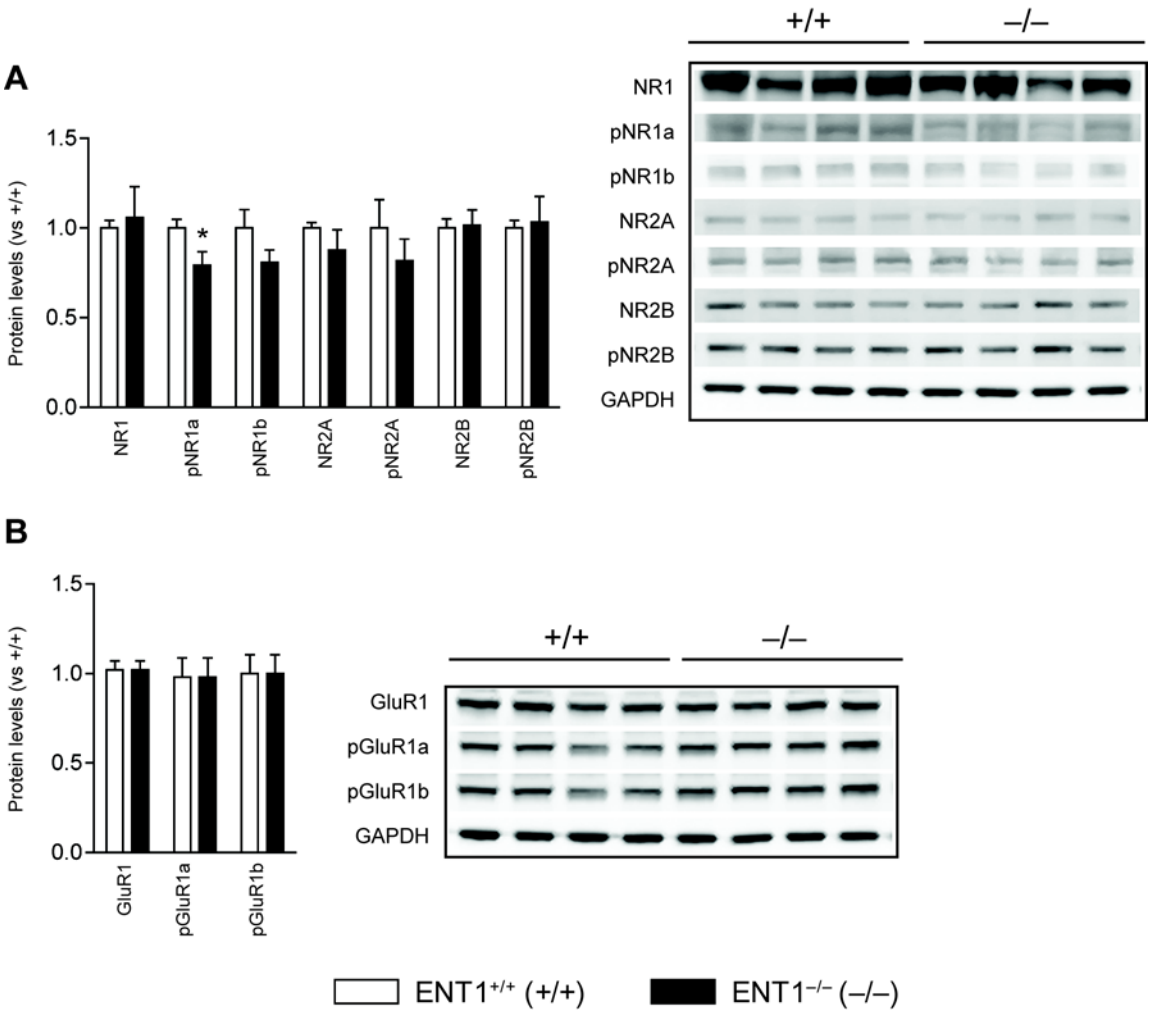

Figure S3. Altered NMDA glutamate receptor (NMDAR) and AMPA glutamate receptor (AMPAR) expressions and phosphorylations in the NAc of ENT1$^{-/-}$ mice. **(A)** Protein expression of NMDAR subunits in the NAc: NR1, pNR1a (Ser890), pNR1b (Ser897), NR2A, pNR2A (Ser1232), NR2B, and pNR2B (Ser1303). Levels of pNR1 (Ser890) were decreased in ENT1$^{-/-}$ mice compared to ENT1$^{+/+}$ mice [$t(17) = 2.7$, $p = 0.016$], while expression levels of other NMDAR subunits were similar in the NAc between genotypes. **(B)** Protein expression of AMPAR subunits in the NAc: GluR1, pGluR1a (Ser831) and pGluR1b (Ser845) were similar between genotypes. $n = 10$ for each genotype; $^{*}p < 0.05$ compared to ENT1$^{+/+}$ mice by unpaired, two-tailed *t*-test. Data are presented as mean ± SEM.

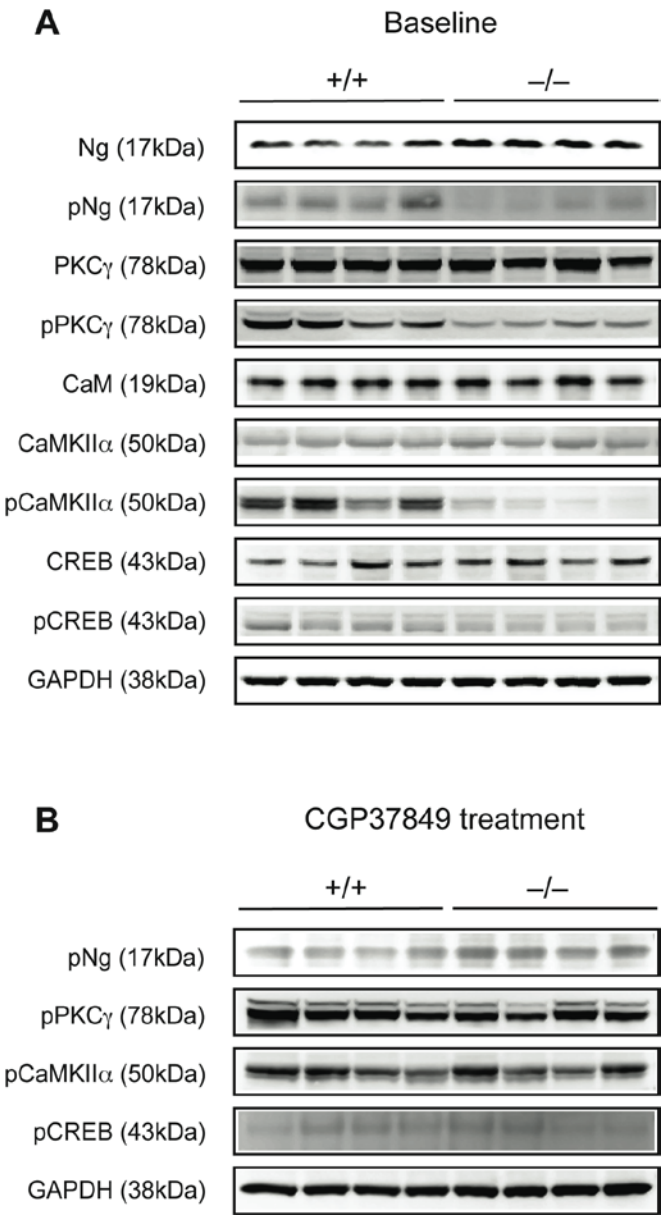

Figure S4. Protein expression of signaling molecules in the nucleus accumbens (NAc). **(A)** Comparison of signaling molecule expression between ENT1$^{+/+}$ and ENT1$^{-/-}$ mice. ENT1$^{-/-}$ mice showed reduced pNg, pPKCγ, pCaMKII and pCREB expression compared to ENT1$^{+/+}$ mice. Representation of phosphoprotein: pNg(Ser36), pPKCγ(Thr514), pCaMKIIα(Thr286), pCREB(Ser133). **(B)** NMDAR antagonist (CGP37849) normalized the reduced phosphoprotein expression in ENT1$^{-/-}$ mice.

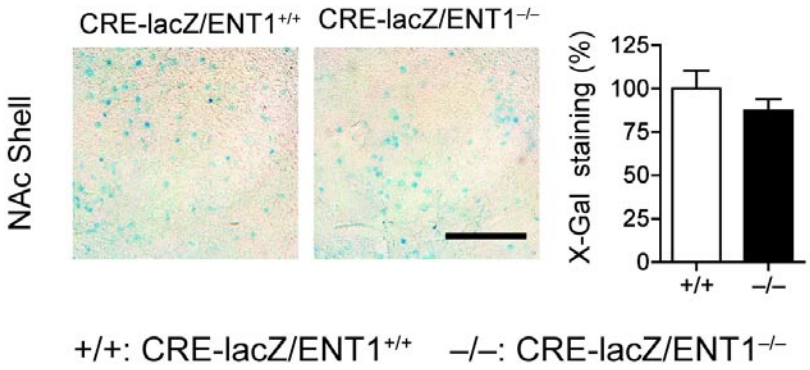

Figure S5. CREB activity in the nucleus accumbens (NAc) shell of CRE-lacZ/ENT1 mice (*n* = 6). Representative coronal brain sections of lacZ expression by X-gal staining in the NAc shell. The positively stained cells by X-gal were similar between genotypes. Scale bar = 100 μm. All data are presented as mean ± SEM.

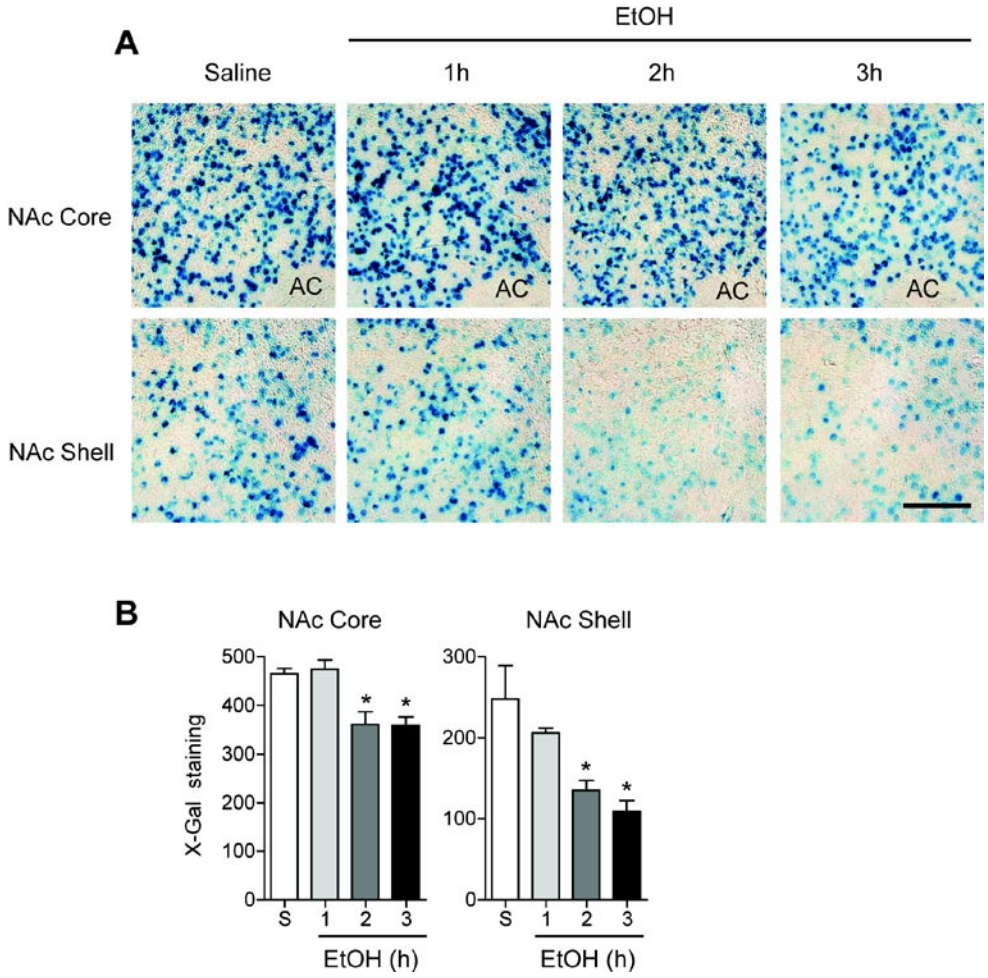

Figure S6. Ethanol treatment reduced the CRE driven b-galactosidase (lacZ) expression in CRE-lacZ mice. **(A)** Representative coronal brain sections of lacZ expression by X-gal staining. Scale bar = 100 μm. **(B)** Positively stained cells by X-gal were significantly decreased in the nucleus accumbens core (NAc Core) [$t(38) = 3.68$, $p = 0.01$ for 2 h, $t(38) = 5.03$, $p = 0.002$ for 3 h], and nucleus accumbens shell (NAc Shell) [$t(38) = 2.61$, $p = 0.03$ for 2 h, $t(38) = 3.19$, $p = 0.01$ for 3 h] after the ethanol (EtOH) treatment (3.0 g/kg, *i.p.*) as compared to the saline (S) treated group. $n = 20$ slides from 4 mice (5 slides/mouse) per treatment; $^*p < 0.05$ compared to the saline-treated group by unpaired two-tailed *t*-test. AC, anterior commissure. All data are the mean ± SEM.

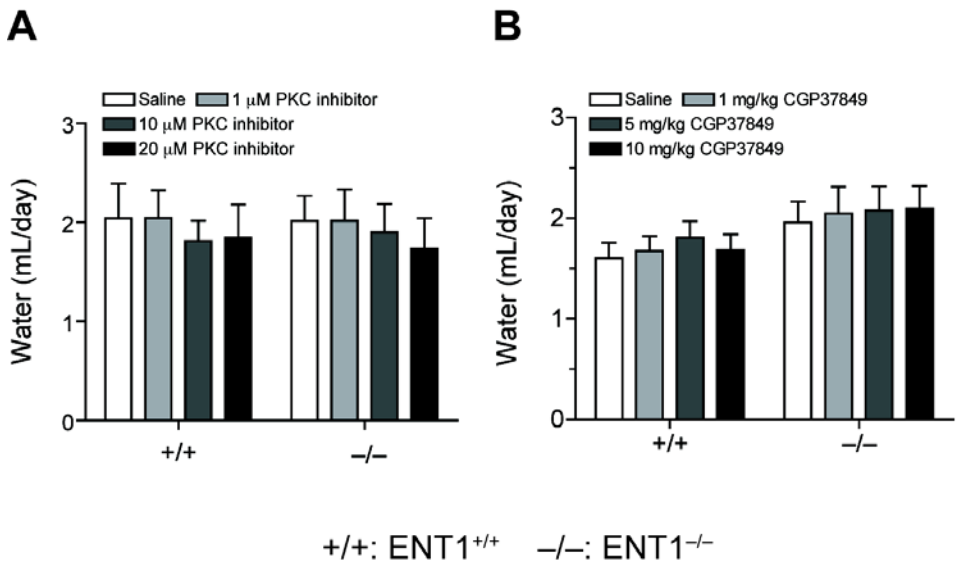

Figure S7. Water consumption of ENT1$^{-/-}$ and ENT1$^{+/+}$ mice. No differences in water consumption (mL/day) between genotypes during a two-bottle choice experiment with **(A)** PKC inhibition (n = 8), or **(B)** CGP37849 treatment (n = 16). Data are presented as mean ± SEM.

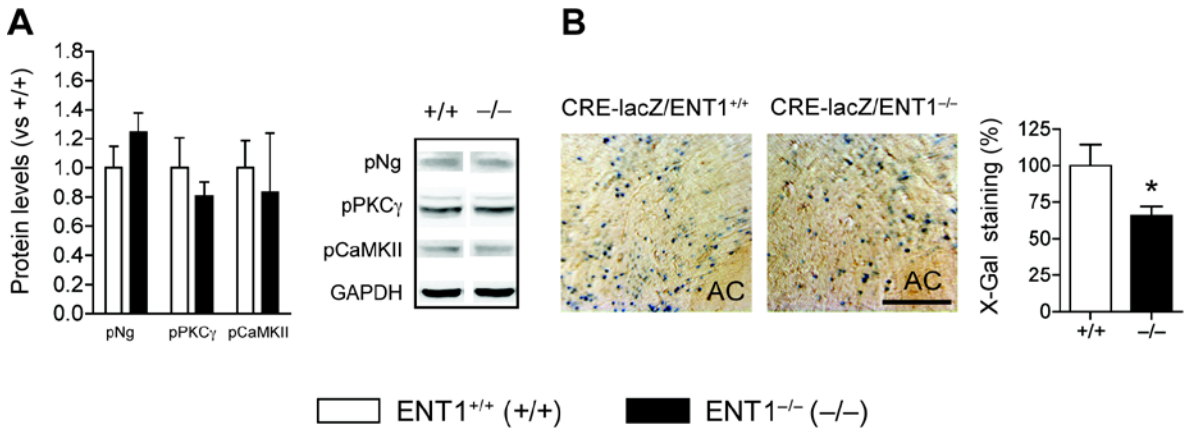

Figure S8. Effects of NMDA receptor antagonist and CAMKII inhibitor on altered signaling molecules in the NAc. CaMKII inhibitor KN93 treatment (15 mg/kg, *i.p.*) blocked the normalization effect of the CGP37849 on CREB activity in NAc of ENT1$^{-/-}$ mice. **(A)** With pre-treatment of KN93, CGP37849 normalized pPKCγ-pNg-pCaMKII signaling. Expression levels are expressed as fold change compared to ENT1$^{+/+}$ mice after normalization with GAPDH. Representation of phosphoprotein: pNg (Ser36), pPKCγ (Thr514), pCaMKII (Thr286). $n = 4$ for each genotype. **(B)** KN93 pre-treatment blocked the normalization effect of the CGP37849 on CREB activity in NAc of ENT1$^{-/-}$ mice. Representative NAc core coronal brain sections of β-galactosidase (lacZ) expression by X-gal staining. Scale bar = 100 μm. Decreased CRE-driven lacZ expression in the NAc core of CRE-lacZ/ENT1$^{-/-}$ mice compared to CRE-lacZ/ENT1$^{+/+}$ mice [$t(35) = 2.22$, $p = 0.03$]. $n = 20$ slides for each genotype; *$p < 0.05$ compared to Cre-lacZ/ENT1$^{+/+}$ mice by unpaired two-tailed t-test. AC, anterior commissure. All data are presented as the mean ± SEM.

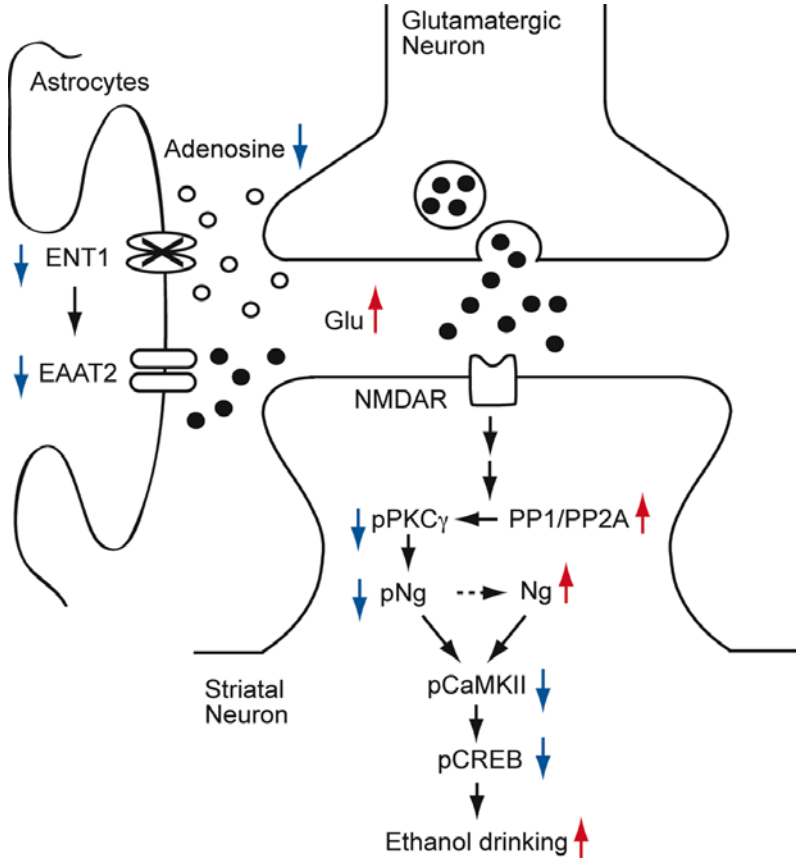

Figure S9. Schematic presentation of a possible signaling mechanism in the nucleus accumbens of ENT1$^{-/-}$ mice. Deletion or inhibition of ENT1 increases glutamate levels by down regulating EAAT2 glutamate uptake activity. Constitutively increased glutamate levels appear to activate phosphatase PP1/PP2A and reduce the active form of PKCγ (pPKCγ-Thr514). Consequently, we found that pNg (Ser36) levels are significantly reduced while total Ng levels are increased. Interestingly, these changes seem to be correlated with the reduction of CaMKII and CREB activities. We confirmed CREB activity using bi-transgenic mice expressing lacZ under the control of the CRE promoter in an ENT1 null background. Reduced CREB activity might increase ethanol drinking in mice lacking ENT1.

References

1. Choi DS, Cascini MG, Mailliard W, Young H, Paredes P, McMahon T, *et al.* (2004): The type 1 equilibrative nucleoside transporter regulates ethanol intoxication and preference. *Nat Neurosci* 7:855-861.
2. Crusio WE, Goldowitz D, Holmes A, Wolfer D (2009): Standards for the publication of mouse mutant studies. *Genes Brain Behav*. 8:1-4.
3. Brodie CR, Khaliq M, Yin JC, Brent Clark H, Orr HT, Boland LM (2004): Overexpression of CREB reduces CRE-mediated transcription: behavioral and cellular analyses in transgenic mice. *Mol Cell Neurosci* 25:602-611.
4. Chen J, Nam HW, Lee MR, Hinton DJ, Choi S, Kim T, *et al.* (2010): Altered glutamatergic neurotransmission in the striatum regulates ethanol sensitivity and intake in mice lacking ENT1. *Behav Brain Res* 208:636-642.
5. Szumlinski KK, Lominac KD, Kleschen MJ, Oleson EB, Dehoff MH, Schwarz MK, *et al.* (2005): Behavioral and neurochemical phenotyping of Homer1 mutant mice: possible relevance to schizophrenia. *Genes Brain Behav* 4:273-288.
6. Che FY, Zhang X, Berezniuk I, Callaway M, Lim J, Fricker LD (2007): Optimization of neuropeptide extraction from the mouse hypothalamus. *J Proteome Res* 6:4667-4676.
7. Bantscheff M, Boesche M, Eberhard D, Matthieson T, Sweetman G, Kuster B (2008): Robust and sensitive iTRAQ quantification on an LTQ Orbitrap mass spectrometer. *Mol Cell Proteomics* 7:1702-1713.
8. Griffin TJ, Xie H, Bandhakavi S, Popko J, Mohan A, Carlis JV, *et al.* (2007): iTRAQ reagent-based quantitative proteomic analysis on a linear ion trap mass spectrometer. *J Proteome Res* 6:4200-4209.

9. House C, Kemp BE (1987): Protein kinase C contains a pseudosubstrate prototype in its regulatory domain. *Science* 238:1726-1728.
10. Chen J, Rinaldo L, Lim SJ, Young H, Messing RO, Choi DS (2007): The type 1 equilibrative nucleoside transporter regulates anxiety-like behavior in mice. *Genes Brain Behav* 6:776-783.
11. Piechota M, Korostynski M, Solecki W, Gieryk A, Slezak M, Bilecki W, *et al.* (2010): The dissection of transcriptional modules regulated by various drugs of abuse in the mouse striatum. *Genome Biol* 11:R48.
12. Choi DS, Wang D, Dadgar J, Chang WS, Messing RO (2002): Conditional rescue of protein kinase C epsilon regulates ethanol preference and hypnotic sensitivity in adult mice. *J Neurosci* 22:9905-9911.
13. Nam HW, Lee MR, Hinton DJ, Choi DS (2010): Reduced effect of NMDA glutamate receptor antagonist on ethanol-induced ataxia and striatal glutamate levels in mice lacking ENT1. *Neurosci Lett* 479:277-281.
14. Vengeliene V, Bachteler D, Danysz W, Spanagel R (2005): The role of the NMDA receptor in alcohol relapse: a pharmacological mapping study using the alcohol deprivation effect. *Neuropharmacology* 48:822-829.
15. Rabbani M, Wright J, Butterworth AR, Zhou Q, Little HJ (1994): Possible involvement of NMDA receptor-mediated transmission in barbiturate physical dependence. *Br J Pharmacol* 111:89-96.
16. Paxinos D, Franklin KBJ (2008): *The Mouse Brain Stereotaxic Coordinates, 3rd ed.* San Diego, CA: Elsevier Academic Press.